Whole-mantle convection and the transition-zone water filter

David Bercovici & Shun-ichiro Karato

Department of Geology and Geophysics, Yale University, PO Box 208109, New Haven, Connecticut 06520-8109, USA

Because of their distinct chemical signatures, ocean-island and mid-ocean-ridge basalts are traditionally inferred to arise from separate, isolated reservoirs in the Earth's mantle. Such mantle reservoir models, however, typically satisfy geochemical constraints, but not geophysical observations. Here we propose an alternative hypothesis that, rather than being divided into isolated reservoirs, the mantle is filtered at the 410-km-deep discontinuity. We propose that, as the ascending ambient mantle (forced up by the downward flux of subducting slabs) rises out of the high-water-solubility transition zone (between the 660 km and 410 km discontinuities) into the low-solubility upper mantle above 410 km, it undergoes dehydration-induced partial melting that filters out incompatible elements. The filtered, dry and depleted solid phase continues to rise to become the source material for mid-ocean-ridge basalts. The wet, enriched melt residue may be denser than the surrounding solid and accordingly trapped at the 410 km boundary until slab entrainment returns it to the deeper mantle. The filter could be suppressed for both mantle plumes (which therefore generate wetter and more enriched ocean-island basalts) as well as the hotter Archaean mantle (thereby allowing for early production of enriched continental crust). We propose that the transition-zone water-filter model can explain many geochemical observations while avoiding the major pitfalls of invoking isolated mantle reservoirs.

The two main sites of mantle upwelling in the Earth are mid-ocean ridges, such as the East Pacific Rise, which draw mantle materials up from shallow depths, and intraplate hotspots, or ocean islands, such as Hawaii, which are possibly due to deep-seated, upwelling plumes. The lavas sampled from these two environments, mid-ocean-ridge basalts (MORB) and ocean-island basalts (OIB), respectively, are in general chemically distinct; that is, MORBs are depleted in incompatible elements including uranium and thorium, while OIBs are relatively enriched in these elements. This suggests that MORB and OIB originate from different source regions.

The terrestrial heat flow also suggests the presence of different source regions. In particular, the approximately 36 TW of heat output from the mantle cannot be produced by a mantle entirely composed of MORB source materials, because it has so few radioactive heat sources; the remaining heat sources are thus thought to be hidden at greater depths in isolated reservoirs unsampled by mid-ocean ridges, but possibly sampled by plumes. In total, these and other observations suggest that the mantle is separated into at least two chemically distinct reservoirs, one depleted by melting processes at ridges, the other relatively enriched and untapped.

Although for many years the 660-km-deep discontinuity was believed to be the barrier between these reservoirs, recent tomographic studies suggested that subducting slabs cross this boundary[1,2] and sink possibly as far as the core–mantle boundary[3]. Other mechanisms for retaining distinct reservoirs have been proposed, including poor mixing (the "plum pudding" model[4]) and placing the boundary between reservoirs near the bottom of the mantle at the D″ layer[5,6]. One of the most recent mantle-layering models[7] places the barrier between reservoirs at about 1,600 km depth; the advantages of this model as opposed to others are discussed in ref. 7. However, whereas the 1,600-km barrier is inferred by the depth at which slabs lose much of their tomographic signature (and are thus presumably stopped) the boundary is not observed in global seismic velocity models[8,9] against which tomographic models are treated as perturbations. This lack of evidence has been attributed to large undulations in the boundary (due to impinging slabs and convective "lava-lamp" type motion[10]), causing an effectively broad, diffuse and hence undetectable boundary. Lack of observation of these undulations in tomography are attributed to the somewhat fortuitous cancellation of chemical and thermal effects in causing seismic velocity anomalies[11].

Layered-mantle models also suffer from dynamical inconsistencies, regardless of whether the boundary between the layers is at 660 km, 1,600 km, or 2,700 km depth. Perhaps most importantly, because any enriched lower layer has most of the heat-producing elements, the depleted overlying layer is heated almost entirely along its base[11]. Basally heated convective systems are characterized by upwelling and downwelling currents with comparable heat transport. However, various analyses of mantle plume heat flow suggest that they account for less than 10% of the net heat flux out of the mantle[12], the remainder being mostly transported by slabs. In general, evidence for slab-dominated convective circulation is very difficult to reconcile with layered-convection models that have a depleted layer basally heated by an underlying enriched one[11].

Although the conflict between geochemical and geophysical constraints has engendered great activity in the mantle dynamics community, the problem remains unresolved, and to some extent—given the ongoing appeal to mantle layering—is no further along than 20 years ago. We propose an alternative hypothesis that avoids the requirement for distinct chemical reservoirs and mantle layering, and explains the observations through a mechanism we term the "transition-zone water filter" (Fig. 1).

Water in the transition zone

The mantle transition zone is the region between the olivine–wadsleyite phase boundary at a depth of 410 km, and the ringwoodite–perovskite/magnesiowüstite transition at 660 km depth, with various other phase transitions in between[13]. Transition-zone minerals have unusual properties relative to upper-mantle minerals, including water solubility[14] and diffusivity of various atomic and electronic species[15,16]. In particular, high-pressure mineral-physics studies have shown that transition-zone minerals at average mantle temperatures have anomalously high water solubility, on the order of 1 wt% (and as much as 3 wt%) whereas the solubility of water in upper- and lower-mantle minerals is less than 0.1–0.2 wt% (refs 17–19). The actual water content in the mantle can be inferred from petrological observations. In particular, volcanic rocks indicate (given estimates for their degree of melting) that the MORB source

region, which is associated with generic upper mantle, is relatively dry with 0.01 wt% water; the OIB source regions, typically presumed to reside in the lower mantle (as we also assume here), are less dry, with around 0.05 wt% water. By comparison, the upper mantle in subduction zones is most enriched in water, with approximately 0.1 wt%, probably due to dehydration of subducting slabs leading to arc volcanism[20].

If either or both upper and lower mantles are near chemical equilibrium with the transition zone (for example, see our model described below), and given that water solubility of the transition zone is about 10–30 times higher than that in the upper and probably lower mantles, then one can estimate a transition-zone water content between 0.1 and 1.5 wt%. Alternatively, various estimates based on planetary accretion models and geochemical mass-balance observations suggest a bulk amount of water in the entire mantle of between three and six ocean masses[21,22]. Neither the upper nor lower mantle can be water-saturated (which would otherwise cause drastic viscosity reductions), and thus the bulk water estimates require the transition zone to have approximately 0.2–2 wt% water (such that the upper and lower mantles are between 0 and 90% of their saturation values). Thus two independent lines of reasoning lead to similar estimates for transition-zone water content that is less than the water saturation limit for transition-zone minerals (3 wt%), but probably exceeds the saturation limit for upper-mantle materials (of order 0.1 wt%; refs 17, 23).

Filtered ambient upwelling mantle

An immediate consequence of the mantle's heterogeneous water-solubility distribution is that, for a wide range of water content, vertical motion across the transition zone results in a dramatic redistribution of both water and trace elements through partial melting. The primary vertical mantle current through which this occurs is the broad background of passively ascending ambient mantle that is forced upward by the downward injection of cold subducting slabs (it is passive in the sense that it rises more from displacement by slabs than under its own buoyancy). Given the small heat and mass flux provided by mantle plumes[12], most of the return flow from slab descent is accommodated by this background upwelling, which is itself only at ambient mantle temperatures and is upwelling at a very slow average velocity of order of magnitude $w_0 \approx 1\ \mathrm{mm\ yr^{-1}}$ (see Methods). This type of circulation is common to convection models and experiments that involve a fluid layer that is heated primarily by distributed heat sources (such as radioactive isotopes), and secondarily by heating along its base[12].

In the upper transition zone, the slowly ascending ambient mantle is in the wadsleyite-dominated assembly (hereafter called 'wadsleyite' for simplicity) and, upon crossing the 410-km boundary, it transforms to an olivine-dominated assembly ('olivine' for simplicity) with significantly lower water solubility. If the wadsleyite below 410 km has water at or in excess of the solubility of olivine above 410 km, as estimated above, then once the ambient upwelling mantle material transforms to olivine it will be saturated, if not super-saturated. At 410-km-deep conditions, the ambient temperature of approximately 1,800 K (ref. 12) is greater than the eutectic point, or wet solidus, of 1,500–1,600 K (ref. 23, 24), and thus the saturated (or super-saturated) ambient mantle will undergo partial melting as soon as it crosses the 410-km boundary[24,25].

Given the extremely small partition coefficients (that is, high incompatibility, or preference for melt over solid) of important trace, incompatible elements, such as uranium and thorium, a melt fraction of only $f \approx 0.5$ wt% is required to reduce the concentration of these elements in the solid phase to MORB source-region

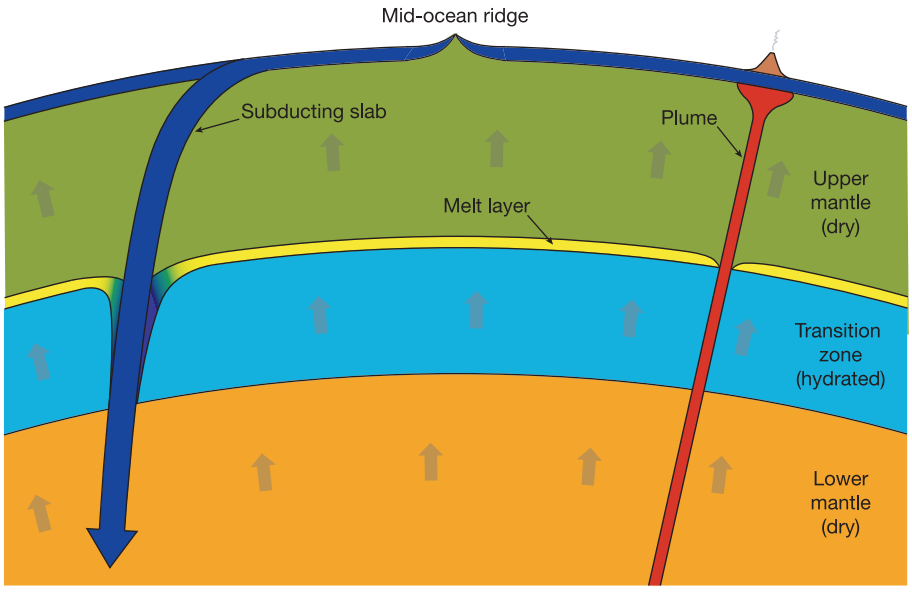

Figure 1 Sketch of the transition-zone water-filter model. Slabs subducting from cold lithosphere (dark blue) force up a broad background of passively upwelling ambient mantle (arrows) that, upon passing through the high-water-solubility transition zone (light blue) gets hydrated. When leaving the transition zone at the 410-km boundary, this ambient mantle becomes low-water solubility olivine and is thus super-saturated, wherein it partially melts, thereby extracting water and filtering off incompatible elements into the melt phase. The wet, enriched melt is likely to be heavy and thus gathers into the high-melt fraction layer trapped above the 410-km boundary (yellow). The residual solid portion of upwelling ambient mantle is buoyant but very dry and depleted of incompatible elements; it provides the MORB source region (green). The water-filtering mechanism is suppressed in mantle plumes (red) due to the plume material's higher temperatures and velocities which result in reduced water-solubility and shorter residence times in the transition zone, thereby leading to greatly diminished hydration and thus little or no melting upon passing the 410-km boundary. Plumes thus arrive at the surface still relatively wet and enriched in compatible elements, thereby providing the source for enriched OIBs. Slabs efficiently entrain the melted material, returning water to the transition zone and incompatible elements to the deeper mantle.

concentrations, that is, a factor of 100 reduction in incompatible-element concentrations[26] (see Methods). Whether melting of ambient upwelling mantle reaches this limit depends on various factors, which we discuss below once the model is completely described.

After partial melting occurs at 410 km, the solid phase will continue to rise, but will be relatively dry and largely filtered of incompatible elements, thereby filling the upper mantle with the water-poor, incompatible-element-depleted material that is sampled by mid-ocean ridges. The remaining water- and incompatible-element-enriched melt residue is likely to be denser than the solid phase because of the melt-solid density crossover that is inferred to exist above the transition zone[27,28] (see Methods). We therefore assume the melts formed at 410 km depth are denser than surrounding solid minerals in the upper mantle but lighter than transition-zone minerals[27,29], in which case they will accumulate and become trapped above the 410-km discontinuity.

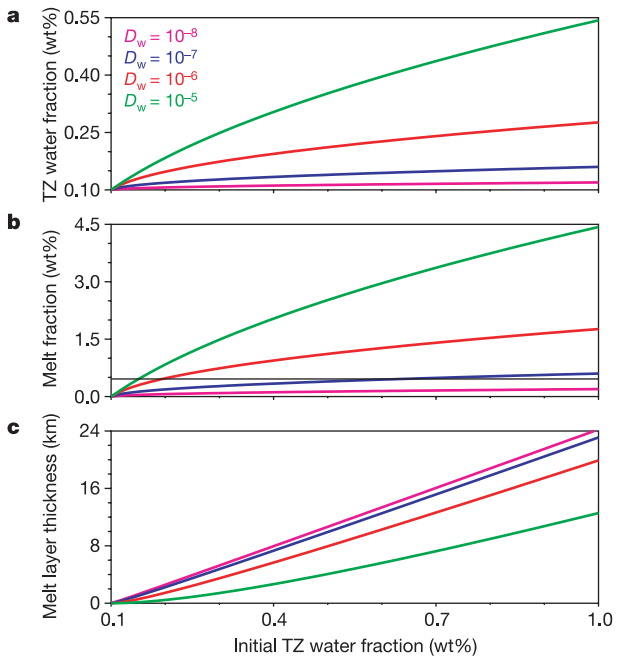

Figure 2 Results of the theoretical model. (See text and Supplementary Information.) **a**, The average water mass fraction of the transition zone (that is, in ambient mantle as it rises out of the transition zone); **b**, the melt fraction *f* of ambient upwelling mantle as it crosses the 410-km boundary; and **c**, the thickness of the resultant melt layer, all shown as functions of initial water content in the transition zone (that is, with no melt layer) and water/hydrogen diffusivity in slabs D_w (in $m^2 s^{-1}$). (See Supplementary section 5 for exact parameter details.) The melt fraction *f* needs to be above approximately 0.5 wt% (thin black line in **b**) to reduce the concentration of uranium (one of the most compatible of incompatible elements, with a partition coefficient of approximately 10^{-3}) in the remaining solid phase by factor of 100 (see Methods). Water or hydrogen diffusivity in wadsleyite at transition-zone conditions is at present unknown. Olivine hydrogen diffusivity is of the order of $10^{-8} m^2 s^{-1}$ (ref. 53); however, diffusion of larger cations in wadsleyite is faster than that in olivine by a factor of 10^3 (ref. 15). Therefore hydrogen diffusivity in wadsleyite is plausibly as much as 1,000 times faster than that in olivine; thus we consider the possible range $10^{-8} m^2 s^{-1} \leq D_w \leq 10^{-5} m^2 s^{-1}$. Higher water diffusivity yields more efficient slab entrainment, in which case only a relatively thin melt layer (that is, smaller slab–melt contact area) is required for slab entrainment to balance melt production. Thus even more water remains in the transition zone rather than the melt layer, leading to larger melt fractions in ambient mantle upwelling across the 410-km boundary. Therefore, cases with higher water diffusivity lead to thinner melt layers and larger melt fractions of ambient upwelling mantle.

Slab entrainment and water recycling

Without any sinks of mass, the trapped melt zone at 410 km would simply continue to accumulate, thicken and spread. However, once the already broad melt layer makes effective contact with cold subducting slabs, its material is readily entrained back into the deeper mantle, thereby draining the melt layer and causing a net, slow flow of melt toward slabs. In particular, a slab extending across the melt layer would cool and re-freeze silicates in its vicinity. In addition to being viscously entrained by the slab, the crystallized materials would be predominantly in the wadsleyite phase and thus also tend to sink under their own weight into the transition zone. The large water-solubility and relatively high water/hydrogen diffusivity of wadsleyite would also permit significant entrainment of water by slabs (see Supplementary section 4). Incompatible elements are also readily returned to the transition zone and lower mantle by slab entrainment; although this entails some elevation of incompatible-element concentrations in the melt layer, especially near slabs, the majority of the incompatible elements remain in the mantle below the 410-km boundary (see Supplementary section 6). Thus the slab entrainment process can, in total, return much of the enriched material back to the deeper mantle.

Most of the water carried by slabs from the melt zone is likely to be eventually deposited in the transition zone. The loss of water from slabs directly to the transition zone is dominated by hydrogen diffusion which is only moderately fast. However, after descending out of the transition zone at 660 km depth, the hydrated minerals entrained by the slab are likely to have water concentrations at the wadsleyite/ringwoodite saturation values (see Supplementary section 4) and thus well in excess of the very low water solubility of the lower mantle. Upon going through the ringwoodite–perovskite/magnesiowüstite phase transition, the slab minerals would be supersaturated and exsolve water, but not induce melting given the reduced slab temperatures and the typically high lower-mantle melting temperatures[30].

The resulting porosity of the matrix holding the exsolved water would be approximately $\rho_s X^*_{wd}/\rho_w = 6\%$ (where $\rho_s \approx 4{,}000\ kg\ m^{-3}$ is silicate density, $\rho_w \approx 2{,}000\ kg\ m^3$ is approximate water density at 660 km depth[31], and $X^*_{wd} = 3$ wt% is the wadsleyite/ringwoodite water saturation mass fraction at slab temperatures) and thus probably of high enough permeability to allow water to percolate back up into the transition zone, where it would be re-absorbed. The return of water to the transition zone by either diffusion or percolation would also be facilitated by the tendency of many slabs to flatten out, permanently or temporarily, in the transition zone at the 660-km boundary[1,2]. Therefore, the production of heavy melts above 410 km and water exsolution beneath 660 km would conceivably lead to water being trapped in the transition zone; without these effects, water could instead be convectively well-mixed over the entire mantle[32].

A simple circulation model

With the inferred trapping and closed circulation of water through the transition zone and overlying melt layer, we can prescribe a simple theoretical model with which to make basic predictions about water concentrations in the transition zone, the melt fraction of ambient mantle upwelling across the 410-km boundary, and the average thickness of the melt layer (Fig. 2). The model is driven by a prescribed background flow of downwelling slabs and the resultant passive ambient upwelling. Given the temperature and water concentration of ambient upwelling, the fraction of melt produced when material crosses the 410-km boundary can be calculated. The flux of silicates, water and incompatible elements injected into the heavy melt layer can then be balanced against their eventual entrainment by slabs back into the transition zone and lower mantle (assuming that all entrained water is deposited in the transition

zone), where they are then recirculated back into the ambient upwelling mantle. See Supplementary Information for model details.

Results of the model (Fig. 2) are cast as functions of the two most poorly constrained parameters: the initial water concentration in the transition zone (that is, before formation of a melt layer), and water diffusivity in wadsleyite, which controls slab entrainment of melt-layer material (see Fig. 2 legend and Supplementary section 5). The model predicts that water in the transition zone is always reduced below its initial value (because it must lose water to the melt layer) and thus remains well below saturation values. The melt fraction of ambient upwelling mantle exceeds the minimum necessary for filtering off incompatible elements (0.5 wt%) if wadsleyite water diffusivity is more than ten times that for olivine, which is plausible. The melt layer thickness varies between 1 km and of the order of 10 km; those cases which have the largest melt fraction and thus best filter off incompatible elements (cases with high water diffusivity) are also associated with the narrowest melt layers (see Fig. 2 legend).

Unfiltered plumes and the Archaean mantle

In contrast to upwelling ambient mantle, the water-filter effect would be largely suppressed in mantle plumes, thus allowing them to deliver moderately enriched mantle material of OIB chemistry to the surface. In particular, upon passing through the transition zone, plume material would conceivably absorb less water than would ambient upwelling mantle.

First, plume material moves with an average velocity on the order of at least $w_{\mathrm{plume}} = 100\,\mathrm{cm\,yr^{-1}}$ (ref. 12). The zone of water entrainment by hydrogen diffusion into the plume is approximated by $\sqrt{D_{\mathrm{w}}H/w_{\mathrm{plume}}}$ where D_{w} is hydrogen diffusivity in the transition zone, and $H = 250\,\mathrm{km}$ is the transition zone thickness. Given a possible range of diffusivity of $10^{-8} \leq D_{\mathrm{w}} \leq 10^{-5}\,\mathrm{m^2\,s^{-1}}$ (see Fig. 2 legend), the entrainment zone is likely to between 300 m and 10 km, which implies that most of the plume (with typical radii of 100 km) remains relatively dry.

Second, recent experimental studies suggest that while water solubility increases with temperature in olivine[33], it decreases with temperature in transition-zone minerals wadsleyite[14] and ringwoodite[34]. Consequently, hot plume material (with temperatures around 2,100 K) passing through the transition zone would have little capacity for water, and would probably be well under-saturated when transforming to olivine above 410 km (see Methods), thus precluding any dehydration melting. Mantle plumes would therefore neither be filtered of their incompatible elements nor stripped of the little water they have. Eventually, upon approaching the surface, the 'damp' plumes would undergo pressure-release melting, leading to hotspots that are wet relative to the much drier MORB, and with enriched OIBs. For similar reasons, the water-filter mechanism could have been suppressed during the Archaean period when temperatures in the Earth were perhaps 200 K higher than today[35] resulting in low transition-zone water concentrations, and thus little or no dehydration-induced melting of mantle material upwelling across the 410 km boundary (Methods). Most of the highly enriched continental crust could therefore have been extracted from the Archaean mantle[36] without impedance from the water-filter mechanism.

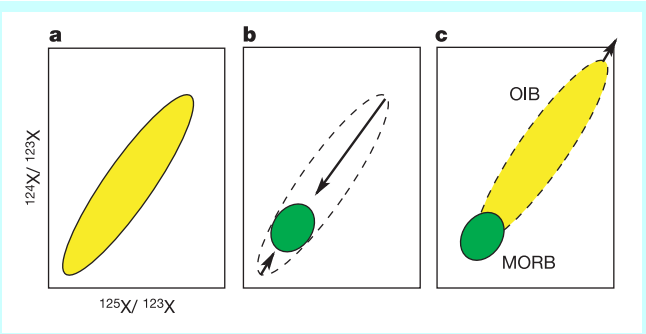

Figure 3 Schematic diagram of MORB and OIB isotopic variation according to the water-filter model. ^{124}X and ^{125}X represent concentrations of generic radiogenic isotopes (such as ^{206}Pb and ^{207}Pb), whereas ^{123}X applies to non-radiogenic ones (such as ^{204}Pb). **a**, Isotopic compositions in mantle below 410 km are heterogeneous, typical for the OIB source region. **b**, Partial melting of ambient mantle above 410 km leads to mixing of these heterogeneous materials in the melt layer; chemical equilibration of the well-mixed melt with the solid phase homogenizes the isotopic composition of the solid to a narrow distribution. The resulting isotopic composition of the solid is a weighted average of isotopic compositions in the deeper region; assuming that either FOZO[4,54] or the Hawaii source region are volumetrically dominant in the deep mantle, the weighted average will be near the depleted end-member composition (**b**). Above 410 km, the depleted solid materials can undergo isotopic evolution for several hundred million to a billion years (given the average 1 mm $\mathrm{yr^{-1}}$ order-of-magnitude velocity of ambient mantle) before reaching mid-ocean ridges. **c**, During this period, the isotopic compositions of the MORB and OIB source materials will shift, leading to present-day observations. The sense of shift is determined by the incompatibilities of parent and daughter elements. If the parent is more incompatible than the daughter (as with U–Pb and Rb–Sr systems)[55] then the MORB source will be relatively depleted in parent elements and undergo less isotopic evolution than will the OIB source (**c**, shift indicated by arrow). However, when the daughter is more incompatible than the parent (as in the Sm–Nd system[55], and possibly the U–He and Th–He systems[37,38]) the opposite trend occurs; the MORB source will grow more enriched in radiogenic isotopes relative to nonradiogenic ones, which may explain the high $^{4}He/\,^{3}He$ for MORB relative to that for OIB).

Geochemical consequences

In addition to their different concentrations of incompatible elements, OIB and MORB source regions also have significantly different isotope ratios (such as between concentrations of radioactive daughter products such as ^{206}Pb to original or primordial ones like ^{204}Pb). The distribution of isotope ratios for OIB is usually much broader than that for MORB, although the two distributions often overlap or are proximal to one another in isotope-ratio space[26]. The difference in distributions is usually attributed to OIB and MORB source regions evolving isotopically in isolation from each other for a billion years or so after formation of the core and crust[26]. However, in our model (Fig. 3), this difference can be attributed to mixing and homogenization of isotope ratios in ambient mantle passing through the hypothetical 410 km melt zone (which causes the MORB distribution to be narrower than, and initially overlap with, the OIB distribution), along with possible drift between the MORB and OIB distributions over a few hundred million to a billion years (also depending on the relative fractionation of parent and daughter isotopes; see Fig. 3).

The abundances of noble gases, such as He and Ar, and their isotopes are also affected by the hypothetical partial melting near 410 km. These elements probably behave like all other highly incompatible elements[37,38] and hence would tend to be sequestered in the deep mantle by the proposed filter mechanism. Therefore the inferred enrichment of the radiogenic isotope ^{40}Ar, as well as its parent ^{40}K, in the deep mantle relative to the MORB source region[39], is naturally explained by our model. The amount of atmospheric ^{40}Ar, which is larger than what can have been generated by the time-integrated amount of ^{40}K in the crust and MORB source region, may be provided by flux of argon from the deep mantle via plumes, as well as extraction from the greater part of the mantle (including deeper ^{40}Ar-enriched portions) during the Archaean[40], before the filter mechanism was activated (see previous section).

The low flux of ^{4}He relative to the global heatflow[41] may be similarly explained in terms of helium incompatibility and partial sequestration in the lower mantle by the filter mechanism. However,

one major limitation of these arguments is the large uncertainty in the partition coefficients of many incompatible elements, especially noble gases, between melts and solids[38]. Moreover, the validity of assumptions behind certain noble-gas constraints can be challenged; for example, assumptions about the K/U ratio in the bulk silicate Earth (which is used to estimate the amount of missing ^{40}Ar and ^{40}K), and the steady-state assumption used in the various noble-gas flux arguments have been recently scrutinized[42,43].

Conclusion

The model presented herein suggests a new form of whole-mantle flow wherein the bulk circulation of mantle material is, via the transition-zone water filter, decoupled from the circulation of incompatible elements. The model therefore explains much of the observations of geochemical reservoirs, including OIB and MORB source regions as well as continental crust, but without invoking layered convection and all its attendant problems. Although our model predicts that the deep mantle is enriched with radioactive elements, the style of convection will be markedly different from that of a layered model which precludes mass transfer between layers. In our model, major-element mass transfer occurs between the two layers, and so the heat generated by radioactive elements in the deep mantle is carried away by a whole-mantle-scale circulation.

One of the predictions of this model is the presence of a layer of melt or partial melt above the 410-km discontinuity, which has also been suggested by other workers[24] but only for the pre-Mesozoic Earth. Obviously, global seismic models[8,9] have not resolved such a melt zone and thus the layer would have to be relatively thin, say less than of the order of 10 km, which is in keeping with the predictions of our model calculations (see Fig. 2). The existence of a melt layer above the 410-km discontinuity has been suggested by recent seismological studies[44,45], although these were focused on particular regions and thus the presence of melt over greater areas is unknown. Further high-frequency body-wave studies and additional coverage offered by large-area land-based and ocean-bottom passive arrays could elucidate whether a thin melt layer above 410 km exists broadly.

Our hypothesis also requires further testing. In particular, aspects of our model hinge on several mineral physics issues which remain highly uncertain. These include the density of hydrous melts at high pressures; diffusivity of hydrogen in transition-zone minerals; water solubility in lower-mantle minerals; temperature-dependence of water solubility in transition-zone minerals; and the partition coefficients of incompatible elements between melt and silicate minerals at transition-zone and deep upper-mantle conditions.

Moreover, sophisticated convection models incorporating the proposed additional physics should shed further light on the feasibility of the mechanism, but will also require considerable technical innovation to treat not only the motion and heat transport of bulk mantle, but also transport of incompatible (most importantly heat-producing) elements, water and partial melts. For now, we leave the transition-zone water filter as an alternative hypothesis to layered convection that can be elaborated on and tested by future geodynamical, seismological, mineralogical and geochemical studies. □

Methods

Rise velocity of ambient upwelling mantle

An important controlling parameter in the water-filter model is the ascent velocity of upwelling ambient mantle as it passes out of the transition zone. This velocity determines, for example, both the rate of production of melts at the 410-km boundary, as well as the transit time for material crossing the upper mantle. Mass conservation across the 410-km boundary requires that upwelling and downwelling volume fluxes balance, that is $2\pi R d_{\mathrm{slab}} w_{\mathrm{slab}} \approx 4\pi R^2 w_0$ where $R \approx 6{,}000$ km is the radius of the 410-km boundary, $d_{\mathrm{slab}} \approx 100$ km is a typical slab thickness, $w_{\mathrm{slab}} = 10\,\mathrm{cm\,yr^{-1}}$ is the order-of-magnitude for a typical slab descent velocity, and w_0 is the average ascent velocity of ambient upwelling mantle. We have assumed that the net plume flux makes a minor contribution and that the net length of the intersection of all slabs with the 410-km boundary is approximately $2\pi R$ because most slabs occur in a nearly great circle around the Pacific rim (and any additional slabs largely compensate for the Pacific rim being slightly smaller than a great circle). This leads to an order-of-magnitude estimate of $w_0 \approx 1\,\mathrm{mm\,yr^{-1}}$, although actual velocities are probably between this and as much as a factor of two smaller.

Melting at the 410-km boundary

Two essential ingredients are needed for the water-filter mechanism to work: (1) a degree of melting of ambient upwelling mantle (as it crosses the 410-km boundary) that is sufficient to filter off incompatible elements; and (2) a resulting melt phase that is heavier than the solid (in order for the melt residue to become trapped at the 410-km boundary until it is entrained by slabs back into the deeper mantle).

Although the melt is presumed heavy and the solid ascends slowly, the diffusivities of incompatible elements such as uranium and thorium are extremely small; thus the melting can be treated as fractional (that is, the phases separate faster than their concentrations of incompatible elements can reach chemical equilibrium). In this case the ratio of incompatible element concentration in the solid phase after partial melting (C_s) to that prior to melting (C_{s0}) is given by $C_s/C_{s0} = (1-f)^{\frac{1}{\Pi}-1}$ (ref. 46) where Π is the partition coefficient between solid and melt. Major incompatible elements, such as uranium and thorium, have $\Pi \approx 10^{-3}$, so to reduce major incompatible elements by a factor of 100 (as is typical for the depletion of the MORB source region[26]) one must have a melt fraction of $f \approx 0.5$ wt%.

The assumption that water- and trace-element-enriched melt is denser than the solid phase is based on the melt-solid density crossover that is inferred to exist in the upper mantle[27–29]. The density crossover, however, has only been investigated for anhydrous melts at high temperatures (for example, ~2,300 K as is relevant for 410 km depths)[29]. The effect of water addition (approximately 10 wt% in the melt[23]; see also Supplementary section 2) on the crossover is at present unknown, but is likely to have a few competing influences. The purely chemical effect of water addition (at the concentrations inferred here) is to reduce melt density; however, since water dissolves in the melt as OH^- as well as molecular water[47–49] the density reduction is relatively small[49,50]: for our model, at most ~5% (calculated from experimental data[49,50]). An equally important effect of water addition is the reduction of melting temperature[23,24]. In particular, the 1,800 K hydrous melt in our model is 500 K cooler than dry melt at equivalent pressure; given that melt thermal expansivity is much larger than that of solids[51,52], the temperature reduction is likely to cause at least a ~5% increase in the melt-solid density difference (relative to 2,300 K conditions). The combined effects are likely to offset each other such that the density crossover occurs in the upper mantle even for our hydrous melt.

Water solubility above and below 410 km

The operation of the water-filter mechanism also depends on the contrast in water-solubility across the 410 km boundary. If the water-solubility of warm or hot upwelling mantle (hotter than the wet-olivine solidus temperature of 1,500–1,600 K) is significantly greater below the 410-km boundary than above it, then the upwelling material can have a wide range of water concentrations that guarantee it will undergo partial melting and subsequent filtering upon crossing the boundary. If the solubility is instead less beneath 410-km than above, then melting is not guaranteed and may even be precluded. The solubility limit $X^\star$ for a given mineral depends on temperature T and pressure P as:

$$X^\star(T,P) = A\varphi(T,P)e^{-\frac{E_a+PV_a}{RT}} \quad (1)$$

where A is a constant, φ is water fugacity, E_a and V_a are the activation energy and volume, respectively, for dissolution of water. All the parameters have been determined for olivine[17,33], and the temperature dependence of water solubility at 410 km can be estimated. The results show that the water solubility in olivine increases with temperature, that is, from less than <0.1 wt% at 1,400 K to ~1 wt% at 2,200 K; at ambient mantle temperatures of 1,800 K this solubility is ~0.2 wt%. The temperature dependence of water solubility in transition-zone minerals is not well known. However, experimental results on ringwoodite[34] show water solubility decreasing with temperature, from ~3 wt% at 1,400 K to ~0.2 wt% at 2,200 K; it is approximately ~1 wt% at 1,800 K. Results for wadsleyite are less robust but a recent compilation of existing data[14] suggests a similar trend: water solubility decreases with temperature. Assuming that the temperature dependence of water solubility in wadsleyite is similar to that of ringwoodite (as with may other properties[15,16] including water-solubility itself), the temperature at which the water solubility in wadsleyite becomes the same as that in olivine is approximately 2,000 K, typical for plumes and Archaean mantle. Thus while there are sufficient conditions for melting of warm present-day ambient mantle, the same is not true of hotter plumes and Archaean mantle. However, melting of mantle upwellings is only precluded if their water concentrations are less than the solidus water concentration, which is generally smaller than the olivine solubility limit. Assuming plume material arises from a relatively dry lower mantle, its water concentrations can remain low enough to avoid melting at 410 km because of the combination of its low water-solubility and short residence time in the 'wet' transition zone. Low water concentrations in the hotter Archaean mantle would conceivably occur because the reduced solubility of the transition zone precludes it from being a water trap, thus distributing water across the mantle.

Received 11 July 2002; accepted 18 July 2003; doi:10.1038/nature01918.

1. Grand, S. Mantle shear structure beneath the americas and surrounding oceans. *J. Geophys. Res.* **99,** 11591–11621 (1994).
2. van der Hilst, R., Widiyantoro, S. & Engdahl, E. Evidence for deep mantle circulation from global tomography. *Nature* **386,** 578–584 (1997).
3. Masters, G., Laske, G., Bolton, H. & Dziewonski, A. in *Earth's Deep Interior* (eds Karato, S., Forte, A., Liebermann, R., Masters, G. & Stixrude, L.) 63–87 (AGU, Washington DC, 2000).
4. van Keken, P., Hauri, E. & Ballentine, C. Mantle mixing: The generation, preservation, and destruction of chemical heterogeneity. *Annu. Rev. Earth Planet. Sci.* **30,** 493–525 (2002).
5. Hofmann, A. & White, W. The role of subducted oceanic crust in mantle evolution. *Carnegie Inst. Wash. Yearbk.* **79,** 477–483 (1980).

6. Coltice, N. & Ricard, Y. Geochemical observations and one layer mantle convection. *Earth Planet. Sci. Lett.* **174,** 125–137 (1999).
7. Kellogg, L., Hager, B. & van der Hilst, R. Compositional stratification in the deep mantle. *Science* **283,** 1881–1884 (1999).
8. Dziewonski, A. & Anderson, D. Preliminary reference earth model. *Phys. Earth Planet. Inter.* **25,** 297–356 (1981).
9. Kennet, B. & Engdahl, E. Travel times for global earthquake location and phase identification. *Geophys. J. Int.* **105,** 429–466 (1991).
10. Davaille, A. Simultaneous generation of hotspots and superswells by convection in a heterogeneous planetary mantle. *Nature* **402,** 756–760 (1999).
11. Tackley, P. Strong heterogeneity caused by deep mantle layering. *Geochem. Geophys. Geosyst.* **3,** 10.1029/2001GC000167 (2002).
12. Schubert, G., Turcotte, D. & Olson, P. *Mantle Convection in the Earth and Planets* (Cambridge Univ. Press, Cambridge, UK, 2001).
13. Ringwood, A. Phase transformations and their bearings on the constitution and dynamics of the mantle. *Geochem. Cosmochem. Acta* **55,** 2083–2110 (1991).
14. Williams, Q. & Hemley, R. Hydrogen in the deep earth. *Annu. Rev. Earth. Planet. Sci.* **29,** 365–418 (2001).
15. Chakraborty, S. *et al.* Enhancement of cation diffusion rates across the 410-kilometer discontinuity in earth's mantle. *Science* **283,** 362–365 (1999).
16. Xu, Y., Poe, B., Shankland, T. & Rubie, D. Electrical conductivity of olivine, wadsleyite, and ringwoodite under upper-mantle conditions. *Science* **280,** 1415–1418 (1998).
17. Kohlstedt, D., Keppler, H. & Rubie, D. Solubility of water in the α, β and γ phases of $(Mg, Fe)_2SiO_4$. *Contrib. Mineral. Petrol.* **123,** 345–357 (1996).
18. Bolfan-Casanova, N., Keppler, H. & Rubie, D. Water partitioning between nominally anhydrous minerals in the $MgO–SiO_2–H_2O$ system up to 24GPa: implications for the distribution of water in the earth's mantle. *Earth Planet. Sci. Lett.* **182,** 209–221 (2000).
19. Murakami, M., Hirose, K., Yurimoto, H., Nakashima, S. & Takafuji, N. Water in earth's lower mantle. *Science* **295,** 1885–1887 (2002).
20. Sobolev, A. & Chaussidon, M. H_2O concentration in primary melts from supra-subduction zones and mid-ocean ridges: implications for H_2O storage and recycling in the mantle. *Earth Planet. Sci. Lett.* **137,** 45–55 (1996).
21. Ringwood, A. *Composition and Structure of the Earth's Mantle* (McGraw-Hill, New York, 1975).
22. Ahrens, T. Water storage in the mantle. *Nature* **342,** 122–123 (1989).
23. Inoue, T. Effect of water on melting phase relations and melt composition in the system $Mg_2SiO_4–MgSiO_3–H_2O$ up to 15GPa. *Phys. Earth. Planet. Inter.* **85,** 237–263 (1994).
24. Kawamoto, T., Hervig, R. & Holloway, J. Experimental evidence for a hydrous transition zone in the early earth's mantle. *Earth Planet. Sci. Lett.* **142,** 587–592 (1996).
25. Young, T., Green, H., Hofmeister, A. & Walker, D. Infrared spectroscopic investigation of hydroxyl in β–$(Mg, Fe)_2SiO_4$ and coexisting olivine: implications for mantle evolution and dynamics. *Phys. Chem. Minerals* **19,** 409–422 (1993).
26. Hofmann, A. Mantle geochemistry: the message from oceanic volcanism. *Nature* **385,** 219–228 (1997).
27. Stolper, E., Walker, D., Hager, B. & Hays, J. Melt segregation from partially molten source regions: the importance of melt density and source region size. *J. Geophys. Res.* **86,** 6261–6271 (1981).
28. Ohtani, E. & Maeda, M. Density of basaltic melt at high pressure and stability of the melt at the base of the lower mantle. *Earth Planet. Sci. Lett.* **193,** 69–75 (2001).
29. Ohtani, E., Nagata, Y., Suzuki, A. & Kato, T. Melting relations of peridotite and the density crossover in planetary mantles. *Chem. Geol.* **120,** 207–221 (1995).
30. Boehler, R. Melting temperature of the earth's mantle and core: Earth's thermal structure. *Annu. Rev. Earth Planet. Sci.* **24,** 15–40 (1996).
31. Pitzer, K. & Sterner, S. Equations of state valid continuously from zero to extreme pressures for H_2O and CO_2. *J. Chem. Phys.* **101,** 3111–3116 (1994).
32. Richard, G., Monnerau, M. & Ingrin, J. Is the transition zone an empty water reservoir? Inferences from numerical model of mantle dynamics. *Earth Planet. Sci. Lett.* **205,** 37–51 (2002).
33. Zhao, Y.-H., Ginsberg, S. & Kohlstedt, D. Experimental investigation on water solubility in olivine single crystals with different Fe content. *Acta Petrol. Sinica* **17,** 123–128 (2001).
34. Ohtani, E., Mizobata, H. & Yurimoto, H. Stability of dense hydrous magnesium silicate phases in the system $Mg_2SiO_4–H_2O$ and $MgSiO_3–H_2O$ at pressures up to 27GPa. *Phys. Chem. Minerals* **27,** 533–544 (2000).
35. Richter, F. Models of Archean thermal regimes. *Earth Planet. Sci. Lett.* **73,** 350–360 (1985).
36. Taylor, S. & McLennan, S. *The Continental Crust: Its Composition and Evolution* (Blackwell, Oxford, UK, 1985).
37. Carroll, M. & Stolper, E. Noble gas solubilities in silicate melts and glasses: new experimental results for argon and relationship between solubility and ionic porosity. *Geochem. Cosmochem. Acta* **57,** 5039–5051 (1993).
38. Chamorro, E. *et al.* Ar and K partitioning between clinopyroxene and silicate melt to 8GPa. *Geochem. Cosmochem. Acta* **66,** 507–519 (2002).
39. Allègre, C., Hofmann, A. & O'Nions, K. The argon constraints on mantle structure. *Geophys. Res. Lett.* **23,** 3555–3557 (1996).
40. Hamano, Y. & Ozima, M. in *Terrestrial Rare Gases* (eds Alexander, E. & Ozima, M.) 155–171 (Japan Scientific Society Press, Tokyo, 1978).
41. O'Nions, R. & Oxburgh, E. Heat and helium in the earth. *Nature* **306,** 429–431 (1983).
42. Albarède, F. Time-dependent models of U–Th–He and K–Ar evolution and the layering of mantle convection. *Chem. Geol.* **145,** 413–429 (1998).
43. Ballentine, C., Van Keken, P., Porcelli, D. & Hauri, E. Numerical models, geochemistry, and the Zero Paradox noble gas mantle. *Phil. Trans. R. Soc. Lond.* **360,** 2611–2631 (2002).
44. Revenaugh, J. & Sipkin, S. Seismic evidence for silicate melt atop the 410-km mantle discontinuity. *Nature* **369,** 474–476 (1994).
45. Vinnik, L. & Farra, V. Subcratonic low-velocity layer and flood basalts. *Geophys. Res. Lett.* **29** doi: 10.1029/2001GL014064 (2002).
46. Shaw, D. Trace element fractionation during anatexis. *Geochem. Cosmochem. Acta* **34,** 237–243 (1970).
47. Burnham, C. in *The Evolution of the Igneous Rocks* (ed. Yoder, J.) 439–482 (Princeton Univ. Press, Princeton, NJ, 1979).
48. Silver, L. & Stolper, E. A thermodynamic model for hydrous silicate melts. *J. Geol.* **93,** 161–178 (1985).
49. Ochs, F. & Lange, R. The partial molar volume, thermal expansivity, and compressibility of H_2O in $NaAlSi_3O_8$ liquid. *Contrib. Mineral. Petrol.* **129,** 155–165 (1997).
50. Richet, P. *et al.* Water and the density of silicate glasses. *Contrib. Mineral. Petrol.* **138,** 337–347 (2000).
51. Fei, Y. in *Mineral Physics and Crystallography A Handbook of Physical Constants* (ed. Aherns, T.) AGU Ref. Shelf 2, 29–44 (AGU, Washington DC, 1995).
52. Suzuki, A., Ohtani, E. & Kato, T. Density and thermal expansion of a peridotite melt at high pressure. *Phys. Earth Planet. Inter.* **107,** 53–61 (1998).
53. Mackwell, S. & Kohlstedt, D. Diffusion of hydrogen in olivine: implications for water in the mantle. *J. Geophys. Res.* **95,** 5079–5088 (1990).
54. Hart, S., Hauri, E., Oschmann, L. & Whitehead, J. Mantle plumes and entrainment: isotopic evidence. *Science* **256,** 517–520 (1992).
55. Hauri, E., Wagner, T. & Grove, T. Experimental and natural partitioning of Th, U, Pb and other trace elements between garnet, clinopyroxene and basaltic melt. *Chem. Geol.* **117,** 149–166 (1994).

Supplementary Information accompanies the paper on **www.nature.com/nature**.

Acknowledgements We thank A. Suzuki and E. Ohtani for access to data and unpublished documents, and G. Leahy for help producing Fig. 1. We also thank A. Hofmann for reviewing the manuscript and R. Batiza, T. Grove, S. Hart, E. Hauri, M. Hirschman, A. Rempel, Y. Ricard, F. Richter, G. Schubert, N. Sleep, D. Stevenson, K. Turekian, L. Vinnik, W. White, and D. Yuen for discussions.

Competing interests statement The authors declare that they have no competing financial interests.

Correspondence and requests for materials should be addresses to D.B. (david.bercovici@yale.edu).